

Loss of Serotonin Oxidation as a Component of the Altered Substrate Specificity in the Y444F Mutant of Recombinant Human Liver MAO A[†]

Ravi K. Nandigama,[‡] J. Richard Miller,[§] and Dale E. Edmondson*

Departments of Biochemistry and Chemistry, Emory University, Atlanta, Georgia 30322-3050

Received May 31, 2001

ABSTRACT: To investigate the roles of tyrosyl residues located near the covalent 8 α -S-cysteinyl FAD in monoamine oxidase A (MAO A) and to test the suggestion that MAO A and plant polyamine oxidase may have structural homology, tyrosyl to phenylalanyl mutants of MAO A at positions 377, 402, 407, 410, 419, and 444 were constructed and expressed in *Saccharomyces cerevisiae*. All mutant enzymes were expressed and exhibited lower specific activities as compared to WT MAO A using kynuramine as substrate. The lowest specific activities in this assay are exhibited by the Y407F and Y444F mutant enzymes. On purification and further characterization, these two mutants were found to each contain covalent FAD. Both mutant enzymes are irreversibly inhibited by the MAO A inhibitor clorgyline and exhibit binding stoichiometries of 0.54 (Y407F) and 0.95 (Y444F) as compared to 1.05 for WT MAO A. Y444F MAO A oxidizes kynuramine with a k_{cat} <2% of WT enzyme and is greater than 100-fold slower in catalyzing the oxidation of phenylethylamine or of serotonin. In contrast, Y444F MAO A oxidizes *p*-CF₃-benzylamine at a rate 25% that of WT enzyme. Steady state and reductive half-reaction stopped-flow data using a series of *para*-substituted benzylamine analogues show Y444F MAO A exhibits quantitative structure activity relationships (QSAR) properties on analogue binding and rates of substrate oxidation very similar to that exhibited by the WT enzyme (Miller and Edmondson (1999) *Biochemistry* 38, 13670): $\log K_d = -(0.37 \pm 0.07)V_w(\times 0.1) - 4.5 \pm 0.1$; $\log k_{\text{red}} = +(2.43 \pm 0.19)\sigma + 0.17 \pm 0.05$. The Y444F MAO A mutant also exhibits similar QSAR properties on the binding of phenylalkyl side chain amine analogues as WT enzyme: $\log K_i = (4.37 \pm 0.51)E_s + 1.21 \pm 0.77$. These data show that mutation of Y444F in MAO A results in a mutant that has lost its ability to efficiently oxidize serotonin (its physiological substrate) but, however, exhibits unaltered quantitative structure–activity parameters in the binding and rate of benzylamine analogues. The mechanism of C–H abstraction is therefore unaltered. The suggestion that polyamine oxidase and monoamine oxidase may have structural homology appears to be valid as regards Y444 in MAO A and Y439 in plant polyamine oxidase.

There is general agreement that the *in vivo* function of monoamine oxidase A (MAO A, EC 1.4.3.4) is to oxidize the neurotransmitter serotonin. Loss of serotonin catabolism by MAO A by gene disruption in either human males (1) or in mice (2) leads to expression of a phenotype of aggressive behavior under stress. Since the crystal structure of this mitochondrial outer membrane-bound enzyme is unknown,

a detailed molecular view of catalytic site amino acid residues remains to be established. With the introduction of a recombinant expression system for human MAO A in *Saccharomyces cerevisiae* (3) and a procedure to purify quantities of the recombinant enzyme sufficient for detailed kinetic and biochemical analysis, it became possible to test various proposals that suggest a structural similarity of MAO A with those of other flavoenzyme amine oxidases.

The elucidation of the 3-dimensional structure of plant polyamine oxidase by Mattevi and his group (4) provided the basis for the suggestion that this enzyme is structurally related to the human MAO's. Subsequently, Wouters and his group have published (5) structural models of MAO A and of MAO B using the coordinates of the plant enzyme and the sequences of the two human enzymes (6, 7). An interesting aspect of these models is the arrangement of two tyrosyl residues on the *re*-face of the isoalloxazine ring of the flavin moiety with a perpendicular orientation of the aromatic rings of the two tyrosyl side chains to the flavin ring (5). This “edge-on” orientation has been shown to result in favorable π – σ interactions between two aromatic rings when there is complementary electrostatic interactions of

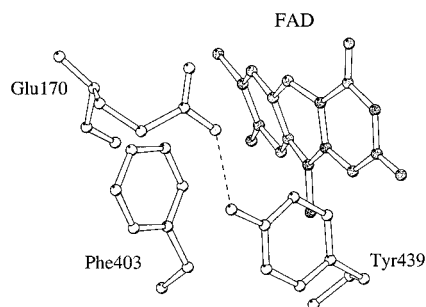
[†] This work was supported by a Grant GM-29433 from the National Institutes of Health (to D.E.E.). R.K.N. received postdoctoral support from the Markey Foundation. J.R.M. received partial support from NIH Predoctoral Training Grant GM-08367.

* To whom correspondence should be addressed at the Department of Biochemistry, Emory University School of Medicine, Rollins Research Center, 1510 Clifton Rd., Atlanta, GA 30322-3050. E-mail: dedmond@bimcore.emory.edu. Phone: 404-727-5972. Fax: 404-727-3452.

[‡] Present address: Department of Microbial Genetics, GlaxoSmith-Kline, Collegeville, PA.

[§] Present address: Pfizer Global Research and Development, Ann Arbor, MI.

¹ Abbreviations: MAO A, monoamine oxidase A.; PAO, polyamine oxidase; WT-MAOA, nonmutated monoamine oxidase A.; QSAR, quantitative structure–activity relationships; k_{red} , limiting rate of enzyme-bound flavin reduction from anaerobic stopped flow experiments.

Scheme 1: Orientation of Tyrosine 439 and Phenylalanine 403 with Respect to FAD in Plant Polyamine Oxidase^a

^a Note that tyrosine 439 is hydrogen bonded to glutamate 170 (taken from PDB No. 1B37).

atoms in the two aromatic rings (8) as expected for tyrosine and flavin. In the case of MAO A, these two tyrosyl residues correspond to Y407 (adjacent to C406 which forms a covalent link to the 8- α -position of the flavin) and to Y444 which is 38 residues toward the C-terminus from the site for covalent linkage. In case of PAO, these aromatic residues correspond to F403 (corresponding to Y407 in MAO A) and Y439 (corresponding to Y444 in MAO A) (Scheme 1). It is of interest that the residue Y444 is conserved in all known MAO A and MAO B sequences from mammals and is present also in the trout MAO sequence (9).

To gain additional insights into the function of these tyrosyl residues that appear to be near the covalent flavin site and, therefore, the catalytic site, we performed a series of conservative mutations of tyrosine to phenylalanine and characterized the respective catalytic activities of the expressed mutant enzymes. The catalytic properties of the Y444F mutant appeared to be of particular interest as regards to the substrate specificity and were subjected to a more detailed kinetic and mechanistic analysis in comparison to those of the WT MAO A. The results demonstrate the importance of tyrosine 444 in a structural role influencing the substrate selectivity of MAO A. QSAR experiments demonstrate that Y444F MAO A exhibits a mechanism identical with that of WT MAO A, however, with altered substrate specificity. The possible role of Y444F mutation in alteration of substrate specificity with loss of serotonin oxidation capability is discussed.

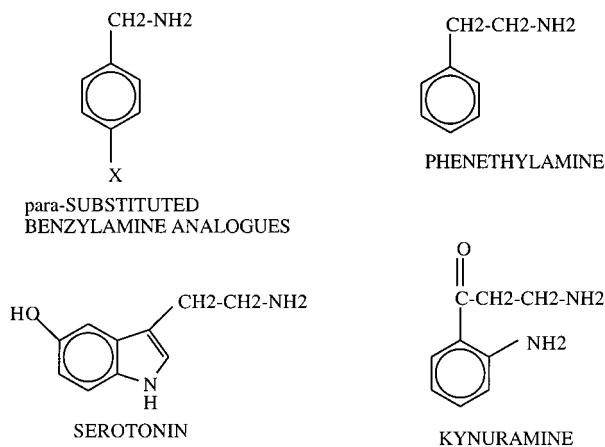
EXPERIMENTAL PROCEDURES

Creation of Site-Specific Mutants of MAO A. The gene encoding human liver MAO A was excised from the pGPD-(G) expression vector (3, 10) by digestion with BamHI. This 1.5 KB fragment was then ligated to a BamHI digested pUC18 to produce pUC18 HMAO A. Site-directed mutants of MAO A were then created using pUC18HMAO A and the transformer site-directed mutagenesis kit (purchased from CLONTECH) as described previously (11). The primers used in creating site-directed mutants of MAO A are listed in Table 1. Incorporation of the desired mutations in the MAO A gene was confirmed by DNA sequence analysis in each case. These mutated MAO A genes were then excised from pUC18 by digestion with BamHI and separated by agarose gel electrophoresis. The purified mutant MAO A genes were then ligated to the BamHI digested expression plasmid, pGPD(G) (10). Proper orientation of the MAO A gene in

Table 1: Primers Utilized for Creating Site-Directed Mutants of Recombinant Human Liver MAO A Expressed in *S. cerevisiae*

| mutant | mutagenic primer |
|--------|----------------------------|
| Y377F | GTGAGCTCTTTGCCAAAGTG |
| Y402F | GTGAGGAGCAGTTCTCTGGGGGCT G |
| Y407F | CTGGGGGCTGCTTCACGGCCTACTTC |
| Y410F | CTACACGGCCTTCTTCCTCCTG |
| Y419F | CATGACTCAATTGGAAGGGTC |
| Y444F | GGAGCGGCTTCATGGAAGG |

Chart 1: Structures of Arylalkylamine Substrates Used in This Work



each case was confirmed by restriction digestion analysis. Plasmids containing properly oriented mutant MAO A were then used to transform *S. cerevisiae* strain RH218 as described (12).

Expression and Purification of MAO A in *S. cerevisiae*. Both wild-type and mutant MAO A forms were expressed in *S. cerevisiae* (RH218). The enzyme preparations were purified to electrophoretic homogeneity from cell pastes obtained from 24 L of culture medium using the procedure described previously (13). *d*-Amphetamine, a competitive inhibitor of MAO A, was used during the final purification step to stabilize the enzyme. Prior to all kinetic experiments, amphetamine was removed by repeated cycles of concentration and dilution of the enzyme sample with amphetamine-free buffer containing 0.8% (w/v) *n*-octyl- β -*D*-glucopyranoside (14).

Substrate Analogues. All the substrate analogues used in this study (structures shown in Chart 1) were either obtained from commercial sources or prepared by reduction of the corresponding benzonitriles as described by Walker and Edmondson (15). *p*-Isopropylbenzylamine was synthesized as described by Hartman and Klinman (16).

Steady-State Kinetic Experiments. All steady-state kinetic experiments were performed at 11 °C in 50 mM potassium phosphate buffer containing 0.8% (w/v) *n*-octyl- β -*D*-glucopyranoside unless otherwise specified. The rates of oxidation of benzylamine analogues were monitored spectrophotometrically at the absorption maxima of the corresponding aldehyde products (15). Steady-state kinetic experiments were performed using a Gilford update of Beckmann DU spectrophotometer or a Perkin-Elmer Lambda 2 spectrophotometer. Competitive inhibition studies for determining the K_i values of several arylalkylamines were performed using *p*-CF₃-benzylamine as the competing substrate. Oxygen uptake studies were performed on a Yellow Springs Oxy-

graph interfaced to a Nicolet 4094 digital oscilloscope which enabled digital acquisition of the rate data. The data were transferred to a PC for data analysis and graphing. The oxygen uptake studies were performed at 25 °C since the responses of the Clark electrode and the membrane in the polarographic detection of O₂ were too slow to permit performing kinetic experiments at 11 °C.

Single-Wavelength Anaerobic Stopped-Flow Kinetic Experiments. Anaerobic stopped-flow experiments were performed using a single-wavelength stopped-flow spectrophotometer (Kinetic Instruments, Ann Arbor, MI). The stopped-flow spectrophotometer is equipped with a 2 cm path-length cell. The apparatus was made anaerobic by incubating the entire flow line and syringes with anaerobic buffer containing 50 mM glucose, 22 nM glucose oxidase, and 100 U/mL catalase for 2–3 h prior to the experiments.

Anaerobic solutions of the enzyme and substrate analogues were prepared in tonometers by repeated degassing and purging with oxygen-free argon (passed over a heated copper chromite catalyst), followed by addition of 50 mM glucose, 22 nM glucose oxidase, and 100 U/mL catalase to remove any traces of remaining oxygen. Anaerobic solutions of enzyme and substrate analogues were mixed via the stopped-flow syringes under pseudo-first-order conditions ($[E] \ll [\text{substrate}]$), and the time-dependent absorption changes at 450 nm were recorded on a Nicolet 4094 digital oscilloscope. The reaction traces were digitally transferred to a PC and analyzed according to single- or double-exponential rate equations with offset.

Data Analysis. Steady-state kinetic parameters were calculated by analyzing the steady-state kinetic data according to the Michaelis–Menten equation using the nonlinear regression analysis program ENZFITTER. The stopped-flow reaction traces were analyzed according to single- or double-exponential rate equations with an off-set using the GRAFIT program. Determination of limiting rates of enzyme-bound flavin reduction and dissociation constants for each amine substrate was performed as described by Strickland et al. (17). Values for the substituent parameters (σ , π , and E_s) were obtained from Hansch et al. (18). Values for the van der Waals volumes (V_w) of each substituent parameter were calculated as described by Bondi (19). Multivariate linear regression analysis of rate and binding data with substituent parameter was performed using the Statview software package (Abacus Concepts).

RESULTS

Comparison of Catalytic and Spectral Properties of Mutants with WT MAO A. Tyrosyl residues about the covalent flavin site (C406) of human liver MAO A were substituted with phenylalanyl residues using standard mutagenesis techniques (11), and the mutated genes were expressed in *S. cerevisiae* strain RH218 under control of a *gal* promoter. Enzyme activities in crude extracts of cell lysates were determined using kynuramine as substrate and the data presented in Table 2. These data demonstrate that kynuramine oxidase activities are observed for all of the mutants tested using the standard MAO A assay conditions. Of particular interest were the comparatively low levels of kynuramine oxidase activities detected for the Y407F and the Y444F mutants of MAO A although immunoblots

Table 2: Specific Activities of MAO A Mutants in Crude Extracts of *S. cerevisiae*

| mutant | specific activity ^a (mU/mg) | mutant | specific activity ^a (mU/mg) |
|--------|---|--------|---|
| WT | 51.1 | Y410F | 21.8 |
| Y377F | 21.4 | Y419F | 30.3 |
| Y402F | 12.1 | Y444F | 0.4 |
| Y407F | 2.8 | | |

^a Activity was measured using 1 mM kynuramine as a substrate in air-saturated 50 mM potassium phosphate buffer (pH 7.5) containing 5 mg/mL reduced Triton X-100 at 30 °C.

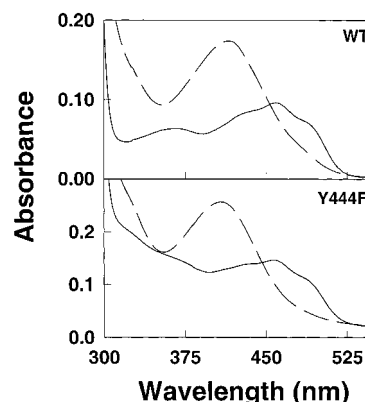


FIGURE 1: UV/visible absorption spectra of purified recombinant WT (8 μ M, top panel) and Y444F (10 μ M, bottom panel) human liver monoamine oxidase A. Solid lines are the spectra of the resting enzymes, and the dashed lines represent the respective spectra after the addition of 8 μ M clorgyline to WT enzyme and 20 μ M clorgyline to the mutant enzyme.

showed comparable levels of enzyme expressed in all mutants under investigation (data not shown). Large-scale cultures (24 L) of yeast strains expressing these two mutants were grown, and the mutant enzymes were isolated using the standard purification procedure for WT enzyme (13).

Figure 1 shows the UV/visible absorption spectra of WT and Y444F MAO A. The absorption spectra of the purified mutant enzyme demonstrates it contains a bound flavin coenzyme. The tendency of the Y407F mutant MAO A to precipitate (even in *n*-octyl- β -*D*-glucopyranoside solution) precluded detailed absorption spectral studies. Electrophoretic and Western blot data (using an antisera specific for covalent flavins (20)) show both the Y407F and Y444F mutant enzyme preparations are homogeneous and that each contains covalently bound FAD (data not shown). Incubation of Y444F MAO A with the MAO A irreversible inhibitor clorgyline results in the formation of a characteristic absorption spectrum of a N(5) flavocyanine structure (Figure 1, bottom panel, dashed line) with subsequent loss of catalytic activity. Incubation of Y407F MAO A with clorgyline also results in the irreversible loss of catalytic activity. The irreversible inhibition of these purified mutant forms of MAO A with clorgyline allowed the determination of their relative levels of functionality by determination of the stoichiometries for inhibition. As shown in Figure 2, 1.05 mol of clorgyline/mol of enzyme-bound flavin inhibits WT MAO A and 0.95 mol of clorgyline/mol of enzyme-bound flavin is required to inhibit Y444 F MAO A. These values are within the experimental uncertainty expected for fully functional enzyme preparation and demonstrate the absence of any detectable levels of inactive enzyme in the Y444F prepara-

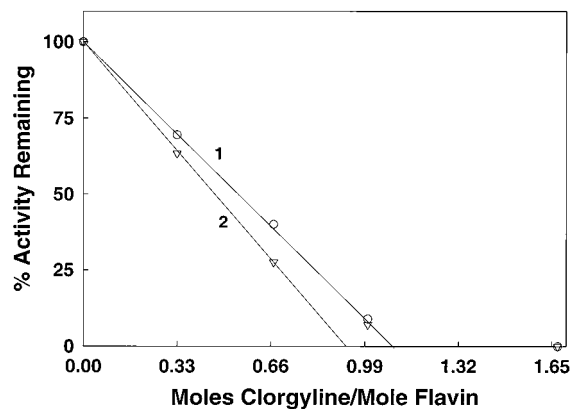


FIGURE 2: Determination of MAO A functionality by titrations with clorgyline. MAO A was incubated with increasing amounts of clorgyline at 4 °C overnight. Residual MAO A activity was determined spectrophotometrically using kynuramine (for WT MAO A) or *p*-CF₃-benzylamine as a substrate (for Y444F MAO A): (1) WT and (2) Y444F.

Table 3: Steady-State Kinetic Parameters of MAO A Mutants Using Kynuramine as a Substrate and MAO A Using *p*-CF₃-Benzylamine as a Substrate^a

| enzyme | k_{cat} (min ⁻¹) | K_m (mM) | k_{cat}/K_m (mM ⁻¹ min ⁻¹) |
|---|---------------------------------------|-------------|--|
| (A) MAO A Mutants Using Kynuramine as a Substrate | | | |
| WT | 125.4 ± 8.5 | 0.13 ± 0.01 | 957 ± 96 |
| Y407F | 42.3 ± 0.7 | 0.16 ± 0.01 | 268 ± 10 |
| Y444F | 1.9 ± 0.1 | 1.72 ± 0.10 | 1.1 ± 0.1 |
| (B) MAO A Using <i>p</i> -CF ₃ -Benzylamine as a Substrate | | | |
| WT | 241.7 ± 5.5 | 0.39 ± 0.03 | 620 ± 24 |
| Y407F | 74.4 ± 1.3 | 0.47 ± 0.02 | 158 ± 12 |
| Y444F | 59.2 ± 0.2 | 1.67 ± 0.12 | 35.4 ± 2.4 |

^a All the kinetic parameters were obtained at 30 °C in air-saturated 50 mM potassium phosphate buffer (pH 7.5) containing 5 mg/mL reduced Triton X-100.

tion. Purified Y407F MAO A is inhibited by 0.54 mol of clorgyline/mol of enzyme-bound flavin which suggests that only half of the enzyme in the preparation has retained catalytic activity on purification. The level of inactive enzyme present in the preparation and its tendency to precipitate even in the presence of detergent precluded determination of the absorption spectrum of clorgyline-modified Y407F MAO A.

Preliminary data with the mutant enzymes show the turnover number is higher when *p*-CF₃-benzylamine is used as a substrate as compared with the activity observed with kynuramine. To further investigate possible alterations in substrate specificity on Y/F mutations, the steady-state kinetic parameters were determined for purified preparations of the two mutant forms of MAO A (correcting for the levels of functional enzyme in each preparation from clorgyline titrations in Figure 2) and compared with those of the purified WT enzyme (Table 3).

The relative k_{cat} values using kynuramine as a substrate show the Y444F mutant exhibits a rate less than 2% that observed with WT enzyme whereas the Y407F mutant is ~1/3 that of WT MAO A. Mutation of Y407 to a F residue did not appreciably alter the K_m value for kynuramine; however, the Y444 F mutant exhibits a >10-fold increase in K_m . In contrast, the kinetic data using *p*-CF₃-benzylamine as substrate shows the Y444 F mutant form of MAO A exhibits a k_{cat} value 24% that of WT MAO A and the Y407 F mutant is 30% that of WT enzyme. The respective K_m

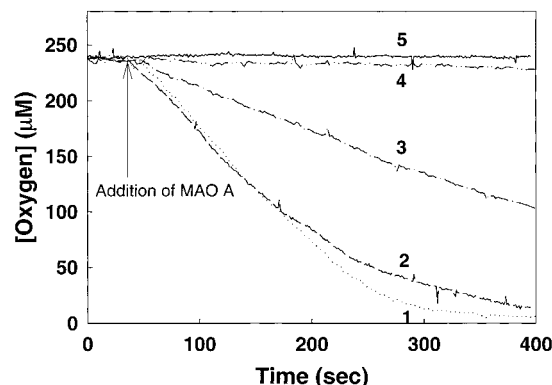


FIGURE 3: Comparative oxidation rates of serotonin and *p*-CF₃-benzylamine by WT MAO A and Y444F MAO A as determined by monitoring O₂ uptake in 50 mM potassium phosphate buffer (pH 7.5) containing 5 mg/mL reduced Triton X-100. Traces 1 and 3 represent the oxidation of 5 mM *p*-CF₃-benzylamine by WT MAO A (0.4 μM) and Y444F MAO A (0.4 μM), respectively. Traces 2 and 4 represent the oxidation of 2.5 mM serotonin by WT MAO A (0.2 μM) and Y444F MAO A (0.2 μM), respectively. Trace 5 represents the background "drift" of the electrode in the absence of any enzyme.

values show the Y444 F mutant exhibits a higher K_m value for this benzylamine analogue than either WT or Y407F MAO A (Table 3). These steady-state data demonstrate that mutation of Y444 to F in MAO A results in a greater alteration in substrate specificity than observed for the Y407F mutant form. The alterations in activity do not result from an increase in the $K_m[\text{O}_2]$ since the observed activity did not increase on increasing [O₂] from air saturation to 100% O₂. The $K_m[\text{O}_2]$ determined from enzyme-monitored stopped flow turnover data is $29.3 \pm 3.2 \mu\text{M}$ for Y444F MAO A catalyzed oxidation of *p*-CF₃-benzylamine, which is similar in value to that of WT MAO A.

Since the Y444 F MAO A mutant exhibits a more dramatic alteration in substrate specificity than does the Y 407 F mutant, the former was examined in detail. It was of interest to determine whether an alteration in substrate specificity is also observed with the physiological substrate serotonin. Any alterations in the active site structure and/or catalytic mechanism might be apparent in changes in QSAR parameters on comparison with WT MAO A (13).

The rates of serotonin oxidation by both WT and Y444 F MAO A preparations were determined polarographically and the results shown in Figure 3. As shown by traces 1 and 3, Y444F MAO A oxidizes *p*-CF₃-benzylamine at a rate ~30–40% that of WT MAO A. When the rate of serotonin oxidation is tested, trace 4 in Figure 3 shows that the rate of O₂ uptake by Y444F MAO A is close to the background drift of the instrument whereas WT MAO A rapidly oxidizes serotonin (trace 2). We estimate the Y444F mutant catalyzes the oxidation of serotonin at a rate ~120-fold slower than WT MAO A ($k_{\text{cat}} = 180 \text{ min}^{-1}$). Unfortunately, the slow rate of oxidation and the tendency of MAO A to exhibit lower activity at high concentrations precluded an accurate determination of steady state kinetic parameters for serotonin oxidation. These results document that the Y444F mutation renders MAO A essentially incapable of catalyzing serotonin oxidation whereas it retains a reasonable level of catalytic efficiency in benzylamine analogue oxidation.

To test the possibility that serotonin is tightly bound to Y444F MAO A but is not oxidized, experiments were

Table 4: Steady-State Kinetic Parameters for the Oxidation of *Para*-Substituted Benzylamine Analogues by Y444F MAO A at 11 °C

| substituent | [α,α]-proteo | | [α,α]-deutero | | kinetic isotope effects | | |
|-------------------|---------------------------------------|------------------|---------------------------------------|------------------|-------------------------|--------------------------|--------------------|
| | k_{cat} (min ⁻¹) | K_m (μ M) | k_{cat} (min ⁻¹) | K_m (μ M) | $^Dk_{\text{cat}}$ | $^D(k_{\text{cat}}/K_m)$ | K_d^a (μ M) |
| CF ₃ | 25.7 \pm 0.50 | 1203 \pm 70 | 2.17 \pm 0.04 | 1200 \pm 0.067 | 11.84 \pm 0.32 | 11.81 \pm 1.01 | 1200 \pm 102 |
| Br | 4.26 \pm 0.05 | 316 \pm 11 | 0.33 \pm 0.01 | 292 \pm 17 | 12.91 \pm 0.42 | 11.93 \pm 0.9 | 290 \pm 22 |
| Cl | 3.07 \pm 0.04 | 493 \pm 23 | 0.19 \pm 0.004 | 354 \pm 26 | 16.16 \pm 0.4 | 11.6 \pm 1.05 | 344 \pm 31 |
| CF ₃ O | 12.8 \pm 0.17 | 307 \pm 18 | 1.19 \pm 0.07 | 568 \pm 0.1 | 10.76 \pm 0.65 | 19.9 \pm 3.88 | 594 \pm 116 |
| I | 11.8 \pm 1.1 | 95 \pm 30 | 0.76 \pm 0.05 | 50 \pm 15 | 15.5 \pm 1.77 | 8.17 \pm 3.68 | 47 \pm 21 |
| F | 1.23 \pm 0.03 | 5676 \pm 398 | ND | ND | ND | ND | ND |
| Me | 1.00 \pm 0.02 | 706 \pm 41 | ND | ND | ND | ND | ND |

^a Calculated from steady-state kinetic isotope effect data. ND: not determined.

Table 5: Kinetic Parameters for the Anaerobic Reduction of Y444F MAO A by *Para*-Substituted Benzylamine Analogues at 11 °C^a

| substituent | [α,α]-proteo | | [α,α]-deutero | | kinetic isotope effect | |
|-------------------|---------------------------------------|------------------|---------------------------------------|------------------|------------------------|--------------------------|
| | k_{red} (min ⁻¹) | K_s (μ M) | k_{red} (min ⁻¹) | K_s (μ M) | $^Dk_{\text{red}}$ | $^D(k_{\text{red}}/K_s)$ |
| CF ₃ | 21.3 \pm 0.37 | 1120 \pm 55 | 2.94 \pm 0.12 | 2324 \pm 270 | 7.24 \pm 0.32 | 15.03 \pm 2.01 |
| CF ₃ O | 13.3 \pm 0.3 | 901 \pm 59 | 1.11 \pm 0.03 | 1067 \pm 89 | 12.46 \pm 0.44 | 14.19 \pm 1.59 |
| Cl | 4.2 \pm 0.07 | 409 \pm 22 | 0.36 \pm 0.02 | 413 \pm 75 | 11.67 \pm 0.67 | 11.78 \pm 2.33 |
| Br | 6.4 \pm 0.16 | 313 \pm 27 | ND | ND | ND | ND |
| F | 1.26 \pm 0.04 | 1956 \pm 298 | ND | ND | ND | ND |
| Me | 0.85 \pm 0.03 | 665 \pm 57 | 0.078 \pm 0.003 | ND | 10.9 \pm 0.57 | ND |
| MeO | 0.23 \pm 0.003 | ND | ND | ND | ND | ND |
| I | 8.8 \pm 0.6 | 318 \pm 55 | ND | ND | ND | ND |
| EtO | 0.34 \pm 0.02 | 348 \pm 60 | ND | ND | ND | ND |
| isopropyl | 0.9 \pm 0.03 | 574 \pm 60 | ND | ND | ND | ND |
| <i>n</i> -butyl | 0.53 \pm 0.004 | ND | ND | ND | ND | ND |

^a ND: not determined.

performed to determine whether it functions as a competitive inhibitor of Y444F MAO A. Using *p*-CF₃-benzylamine as a substrate, no inhibition of catalytic activity is observed at serotonin concentrations up to 1 mM. This property is in contrast to that of the native enzyme in which a K_s value = 230 μ M is determined from reductive half-reaction experiments. Therefore, serotonin does not bind to the mutant enzyme with any significant level of affinity. The ability of Y444F MAO A to oxidize phenethylamine was tested by measuring the rate of enzyme-bound flavin reduction in the stopped-flow apparatus under anaerobic conditions. In the presence of 10 mM phenethylamine, the mutant enzyme is reduced at a rate of 2×10^{-3} min⁻¹, which is 400-fold slower than the limiting rate of enzyme reduction (k_{red}) exhibited by the WT enzyme (14). Therefore, the altered substrate specificity of Y444F extends to those substrate analogues which contain an ethyl side chain. The nature of the aromatic ring does not appear to be the sole determinant in substrate specificity alteration.

QSAR Studies of Benzylamine Analogue Binding and Rate of Oxidation with Y444F MAO A. The above data demonstrate that the Y444F mutation alters the substrate specificity of MAO A. Therefore, it was of interest to determine whether the QSAR parameters relating to benzylamine *para*-substituent parameters (13) on substrate binding and on the rate of C–H bond cleavage had been altered on this mutation. In addition, recent work has also identified a QSAR correlation of alkylamine side chain contributions to the affinity of arylalkylamine analogue binding to the active site of MAO A (14) and it was of interest to determine if this correlation is altered with the mutant enzyme. Steady-state and reductive half-reaction stopped-flow kinetic approaches were performed with Y444F MAO A that have been previously applied to WT MAO A in this laboratory (13, 14). The steady-state and deuterium kinetic isotope effect

data are presented in Table 4. All analogues exhibit steady-state kinetic properties with Y444F MAO A that follow Michaelis–Menten kinetic behavior. Large $^Dk_{\text{cat}}$ and $^D(k_{\text{cat}}/K_m)$ values are observed for several *para*-substituted benzylamine analogues and are somewhat larger in value than those observed with WT enzyme (13). The slower rate of oxidation of these analogues by the mutant enzyme probably leads to lower commitment factors and a more complete expression of the kinetic isotope effects. The slow rates of oxidation of *p*-F- and *p*-Me-benzylamine analogues precluded the determination of Dk values for these analogues. Using the procedure published by Klinman and Matthews (21), the K_d values for benzylamine analogue binding to Y444F MAO A were calculated (Table 4).

Reductive half-reaction data were obtained at various substrate analogue concentrations using the stopped-flow spectrophotometer under anaerobic conditions, and the data were analyzed by the method of Strickland et al. (17) as done previously (13, 14). The limiting rates of flavin reduction of Y444F MAO A by the *para*-substituted benzylamine analogues (Table 5) exhibit close agreement with the k_{cat} and deuterium kinetic isotope effect values and are similar to those determined in steady-state experiments. Therefore, the rate limitation in catalysis for Y444F MAO A oxidation of benzylamines is demonstrated to be C–H bond cleavage as concluded from similar experiments with WT MAO A (13). No spectrally observable kinetic intermediates are observed in stopped-flow studies on Y444F MAO A using either α,α -¹H- or α,α -²H-labeled substrates.

The influence of substituent parameters on the binding affinities and rates of flavin reduction of Y444F MAO A by the series of *p*-X-benzylamine analogues were analyzed using the equation

$$\log K \text{ (or } k) = \sigma\rho + A\pi + BV_w \text{ (or } E_s) + C \quad (1)$$

Table 6: Correlations of the Binding Affinities (K_s or K_d) of Deprotonated *Para*-Substituted Benzylamines for Y444F MAO A with Steric, Electronic, and Hydrophobic Substituent Parameters^a

| param | correlation | | corr coeff | F^b value | significance ^c |
|----------------|------------------|------------------|---------------|----------------|---------------------------|
| | slope | y intercept | | | |
| π | -0.39 ± 0.30 | -4.84 ± 0.11 | 0.17 | 1.7 | 0.2326 |
| σ | 0.28 ± 0.49 | -5.16 ± 0.12 | 0.04 | 0.3 | 0.5915 |
| E_s | 0.60 ± 0.15 | -4.36 ± 0.17 | 0.76 | 15 | 0.0112 |
| V_w | -0.37 ± 0.07 | -4.50 ± 0.13 | 0.77 | 27 | 0.0009 |
| $V_w + \pi$ | -0.37 ± 0.09 | -4.50 ± 0.13 | 0.77 | 12 | 0.0059 |
| | -0.01 ± 0.19 | | | | |
| $V_w + \sigma$ | -0.37 ± 0.07 | -4.54 ± 0.13 | 0.80 | 14 | 0.0038 |
| | 0.24 ± 0.24 | | | | |

^a K_s values used in linear regression analysis were obtained from proteo and dideutero benzylamine analogues. K_d values were calculated from steady-state isotope effects as described by Klinman and Mathews (21). All values are corrected to reflect the selective binding of the deprotonated amines to the enzyme according to eq 2. Correlations do not include (*p*-trifluoromethyl)- and (*p*-isopropylbenzyl)amine. ^b The F value is a statistical term relating the residual of each point to the fitted line to the residuals of each point to the mean value. F is weighted for the number of variables in the correlation and the number of data points. A higher F value indicates a better fit. ^c Significance is calculated from the F value and represents the fractional chance that the derived correlation is meaningless.

where K is the binding affinity of the benzylamine analogue determined from either steady-state kinetic isotope effect data (21) or from the K_s value determined from reductive half-reaction stopped-flow data (17) and k is the rate of oxidation of the benzylamine analogues under steady-state conditions (k_{cat}) or the limiting rates of flavin reduction during reductive half-reaction (k_{red}). The σ value is the electronic parameter of the substituent (18), π is the hydrophobicity of the substituent (22), and the steric parameter can be represented by either V_w (the van der Waals volume of the substituent (19)) or by E_s (the Taft steric parameter (23)). The apparent binding constants from Tables 4 and 5 were corrected to account for binding of only the deprotonated form of the amine analogue (24) using the equation

$$K_d(\text{deprotonated}) = \frac{K_d(\text{observed})}{1 + \text{antilog}(pK_A - \text{pH})} \quad (2)$$

The binding data were subjected to linear regression analysis with either single- or two-substituent parameter correlations shown in Table 6. From the data available, the best correlation to describe *p*-X-benzylamine binding to Y444F MAO A is a single correlation with the steric parameter V_w in accord with the relation

$$\log K_d = -(0.37 \pm 0.07)V_w(\times 0.1) - 4.5 \pm 0.1 \quad (3)$$

which is similar but not identical with the correlation determined for the WT MAO A (13):

$$\log K_d = -(0.45 \pm 0.05)V_w(\times 0.1) - 4.8 \pm 0.1 \quad (4)$$

A plot describing this relation is shown in Figure 4. Note that as observed for WT MAO A, the *p*-CF₃ and *p*-isopropyl substituents are outliers from the other substituents in the linear correlation. The molecular basis for their being outliers is not known. It may reflect steric effects of the *p*-isopropyl substituent and H-bonding of the *p*-CF₃ substituent which would modify their respective electronic effects on C–H

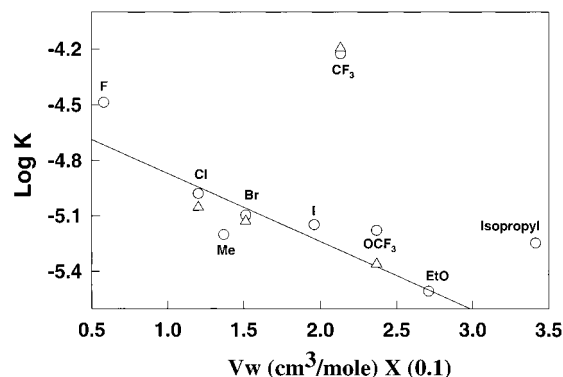


FIGURE 4: Correlation of benzylamine analogue binding to Y444F MAO A with van der Waals volume (V_w) of *para* substituents. Note that *p*-CF₃-benzylamine and (*p*-isopropyl)benzylamine analogues are not included in the analysis. The solid smooth line is the linear best fit of the experimental data. The binding constants were obtained as K_s (17) from pre-steady-state kinetic experiments or as K_d (21) from steady-state kinetic isotope effect data.

Table 7: Correlations of the Reductive Half-Reaction Rate Data of Y444F MAO A and *Para*-Substituted Benzylamine Analogues with Steric, Electronic, and Hydrophobic Substituent Parameters^a

| param | correlation | | corr coeff | F value | significance |
|----------------|------------------|------------------|---------------|--------------|--------------|
| | slope | y intercept | | | |
| π | 0.31 ± 0.31 | 0.21 ± 0.29 | 0.06 | 1.0 | 0.3200 |
| σ | 2.43 ± 0.19 | 0.17 ± 0.05 | 0.91 | 160 | <0.0001 |
| E_s | -0.64 ± 0.22 | -0.40 ± 0.31 | 0.40 | 8.7 | 0.0115 |
| V_w | -0.06 ± 0.17 | 0.57 ± 0.36 | 0.01 | 0.1 | 0.735 |
| $\sigma + \pi$ | 2.39 ± 0.18 | 0.05 ± 0.09 | 0.92 | 91 | <0.0001 |
| | 0.15 ± 0.09 | | | | |
| $\sigma + E_s$ | 2.09 ± 0.25 | 0.06 ± 0.11 | 0.92 | 62 | <0.0001 |
| | 0.20 ± 0.10 | | | | |
| $\sigma + V_w$ | 2.47 ± 0.19 | 0.05 ± 0.11 | 0.92 | 83 | <0.0001 |
| | 0.06 ± 0.05 | | | | |

^a Correlations include both k_{cat} and k_{red} , taken from Tables 4 and 5.

bond cleavage step. Thus, the conclusion from these studies is that mutation of Y 444 to a phenylalanine does not appreciably influence the binding of benzylamine analogues to the substrate binding site although the intrinsic binding affinity is somewhat weaker than observed with unmodified enzyme.

Previous QSAR studies on MAO A demonstrated the rate of flavin reduction and of k_{cat} for differing *p*-X-benzylamine analogues were dependent only on the electronic parameter of the *para* substituent (13) ($\rho = +2$) which provided strong evidence for a H⁺ abstraction mechanism as the mode of C–H bond cleavage. Analysis of similar data for Y444F MAO A in Table 7 and in Figure 5 demonstrates this relation is also observed in the mutant enzyme where the best correlation of substituent effect on rate is with the electronic contribution

$$\log k = +(2.43 \pm 0.19)\sigma + 0.17 \pm 0.05 \quad (5)$$

which also supports the mode of C–H bond cleavage follows a H⁺ abstraction mechanism. Thus, the QSAR data on Y444F MAO A demonstrate this mutation does not have a large influence on either the mode of benzylamine binding or the mechanism of the C–H bond cleavage step.

QSAR Studies of Alkyl Side Chain Contribution to Binding to Y444F MAO A. The activity of the mutant enzyme is more affected when substrates with ethyl alkyl side chains (includ-

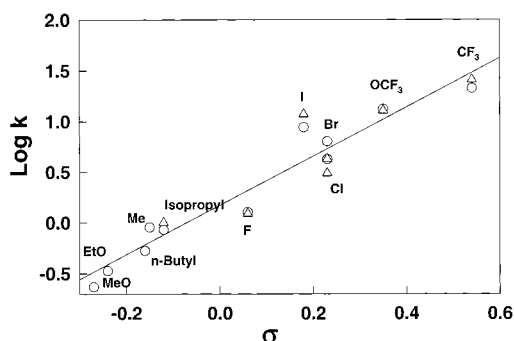


FIGURE 5: Correlation of the rate of benzylamine oxidation by Y444F MAO A with electronic parameter (σ) of para substituents. The solid smooth line is the linear best fit of the experimental data. The rate of benzylamine oxidation was obtained either as a steady-state turnover rate (k_{cat}) or as a rate of reduction of enzyme-bound flavin under anaerobic conditions (k_3 , 17).

Table 8: Inhibition Constants for Arylalkylamine Analogue Binding to Y444F MAO A^a

| arylalkylamine | $K_i(\text{obsd})$ (μM) | $K_i(\text{corr for p}K_a)$ (μM) ^b |
|--------------------------|--------------------------------------|--|
| benzylamine ^c | 3360 ± 540 | 49.0 ± 7.9 |
| phenethylamine | 6740 ± 100 | 33.6 ± 0.5 |
| (3-phenylpropyl)amine | 643 ± 211 | 3.21 ± 1.05 |
| (4-phenylbutyl)amine | 223 ± 22 | 1.11 ± 0.11 |
| amphetamine | 69.4 ± 15.8 | 0.35 ± 0.08 |

^a K_i values were determined using *p*-CF₃-benzylamine as a competing substrate. ^b The values denoted are corrected for the concentration of the deprotonated form of the amine analogues. ^c α, α -[²H]-benzylamine was used as an inhibitor to determine the K_i value.

ing kynuramine, phenethylamine, or serotonin) are tested. Recent work from this laboratory on WT-MAO A (14) has identified a correlation of the E_s of the alkyl side chain of arylalkylamines with their respective binding affinities according to the correlation (14)

$$\log K_d = (4.11 \pm 0.56)E_s + 0.24 \pm 0.97 \quad (6)$$

which quantifies the steric influence of the alkyl side chain as a strong contributor to the binding affinity of these arylalkylamines to MAO A. To examine whether the Y444F mutation alters this relationship, the K_i values of a series of arylalkylamines were tested. Since benzylamine is a weak substrate for this mutant enzyme, the binding affinity was determined by using the α, α -[²H] analogue as a competitive inhibitor of *p*-CF₃-benzylamine oxidation. The other compounds tested (phenethylamine, 3-phenylpropylamine, 4-phenylbutylamine, and *d*-amphetamine) are also found to be competitive inhibitors, and their respective K_i values were determined accordingly (Table 8). The respective observed binding affinities were corrected for the selective binding of the deprotonated form of the amine (see eq 2) and the data correlated with the Taft steric parameter (E_s) of the alkyl side chain according to the equation

$$\log K_i = (4.37 \pm 0.51)E_s + 1.21 \pm 0.77 \quad (7)$$

The plot describing this equation correlation is shown in Figure 6. Note that the above correlation is similar to that observed with WT MAO A, which demonstrates that the mutation of Y 444 to F does not materially alter the influence of E_s of the aryl side chain on the binding affinity of the amine to MAO A.

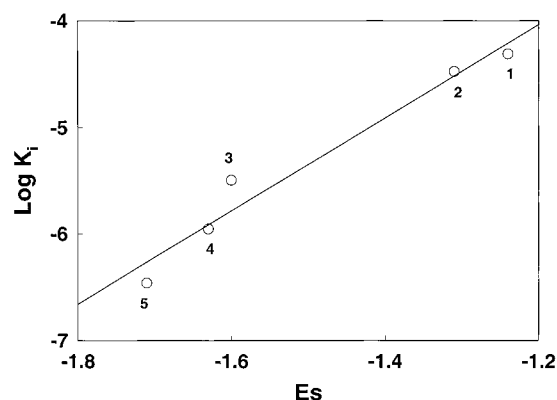


FIGURE 6: Correlation of arylalkylamine binding to Y444F MAO A with steric parameter (E_s) of alkyl side chain of the analogues. The binding affinities of the arylalkylamine analogues are measured as K_i using *p*-CF₃-benzylamine as competing substrate. The arylalkylamines used in this study are as follows: 1, α, α -[²H]-benzylamine; 2, phenethylamine; 3, (3-phenylpropyl)amine; 4, (4-phenylbutyl)amine; 5, *d*-amphetamine. The solid smooth line is the linear best fit of the experimental data.

DISCUSSION

The results in this paper demonstrate the creation of a mutant form of MAO A that is no longer able to efficiently oxidize its physiological substrate, serotonin, but retains its ability to oxidize the benzylamine class of substrates. Therefore, this mutated form of MAO A may be of interest in cell system studies where impairment of serotonin catabolism is desired in lieu of deletion of MAO A completely. The results in this study also point out the utility of monitoring differing amine substrates in assaying the functional consequences of MAO mutations to avoid reaching erroneous conclusions. For example, upon comparison of the activities of mutant enzymes in crude cell lysates using kynuramine as a substrate (Table 2), it appears that Y444F mutant retained <1% catalytic activity of that of WT MAO A. However, upon closer examination using the purified forms of Y444F MAO A, it is apparent that the mutant enzyme retains ~30% activity of that of WT MAO A using *p*-CF₃-benzylamine as substrate. Therefore, caution should be exercised while comparing the activities between wild-type and mutant enzymes on the basis of the data using a single substrate.

Mutation of Y444 to F in MAO A is shown not to interfere with the covalent flavinylation of the enzyme. This is shown in Figure 1 where the absorption spectrum of the mutant enzyme is typical of the bound FAD cofactor. The enzyme is fully functional on the basis of clorgyline titrations. Immunoblot experiments demonstrate that FAD is covalently linked to Y444F MAO A. The enzyme appears to fold in the correct manner since the mutant form retains the QSAR properties of WT enzyme with respect to benzylamine analogue binding and substituent influence on the rate of oxidation. The binding parameters show that the site for binding of the phenyl ring of the substrate is not altered to any large extent in the mutant and the rate correlation provide further support for the mechanism of C–H bond cleavage in catalysis as a H⁺ abstraction.

The major effect of loss of the OH group from Y444 in MAO A is its inability to efficiently catalyze the oxidation of phenethylamine and of serotonin. Both substrates are

oxidized by Y444F MAO A at rates >2 orders of magnitude slower than WT enzyme. No binding of serotonin to Y444F MAO A is observed up to a concentration of 1 mM (a concentration 4-fold higher than the K_S value observed for serotonin binding to the native enzyme). In the case of phenethylamine binding, a 4-fold decrease in observed binding affinity is observed when compared to WT. It should be noted that the binding affinities of all the benzylamine analogues toward Y444F MAO A are 2–3-fold weaker than those observed for WT MAO A. The binding data and correlations (Table 8 and Figure 6) show results similar to that of WT MAO A. Thus, the binding interaction(s) of the alkyl side chain is similar in both WT and Y444F MAO A and hence the 2–3-fold weaker binding of benzylamine analogues or phenethylamine originate from a slightly altered binding pocket for the phenyl ring within the substrate binding site of Y444F MAO A. Thus, the alkyl side chain binding interactions are not influenced by replacing Y444 with F. However, it is interesting to note that whereas phenethylamine is an excellent substrate for WT MAO A, it is oxidized ~ 2 orders of magnitude slower by Y444F MAO A, albeit with reasonable binding affinity.

The inability of the mutant enzyme to efficiently oxidize phenethylamine and serotonin and the lack of any apparent binding affinity for serotonin can be explained in the following manner. Loss of “OH” group upon mutating Y444 to F could disrupt a site for hydrogen bonding of this residue to other H-bonding acceptor(s) in the enzyme (in PAO, the corresponding tyrosine is hydrogen bonded to a glutamate residue, Scheme 1 (4)). Thus the aromatic ring of F444 in the mutant enzyme might assume different conformational states resulting in an altered binding pocket for the aromatic ring of substrate analogues. This altered substrate binding pocket may lead to altered binding modes which may not accommodate the bulky aromatic hydroxyindole ring of serotonin and, thus, results in a very weak binding of serotonin to Y444F MAO A and 2–4-fold weaker binding of benzylamine analogues and phenethylamine.

In case of phenethylamine, the increased steric flexibility of the longer alkyl side chain coupled with altered aromatic ring orientation may result in the formation of a nonproductive complex which results in this amine being a reasonably competitive inhibitor for Y444F MAO A. Arylalkylamine analogues with long flexible alkyl side chains are known to inhibit MAO A due to the formation of nonproductive complexes (14). Preliminary stopped-flow data in this laboratory show the presence of two kinetic phases of flavin reduction on reaction with WT recombinant human MAO A with serotonin. The rapid phase may result from a “productive” binding mode of serotonin in the active site while the slow phase may result from a “nonproductive” mode of serotonin binding. A more complete investigation of this interaction is currently under investigation in this laboratory.

In conclusion, the results of this study shows that a Y444F mutation in MAO A results in alterations in substrate specificity that are dependent on the size of the aromatic ring and on the length alkyl side chain of various substrate analogues. The data verify the importance of Y444 as a component of the substrate binding site even though it is 38 residues toward the C-terminus from the residue C406 which covalently binds the FAD cofactor.

The suggestion of a structural similarity of plant polyamine oxidase with that of MAO is supported by the work reported here. Therefore, residue Y439 in plant polyamine oxidase may be considered to be structurally homologous with Y444 in MAO A. Since structural studies suggest this residue to form a part of the channel for substrate contact with flavin ring as required for catalysis in PAO, this may also be a role for Y444 in MAO A. Therefore, it would be of interest to mutate Y439 to F in PAO and examine the influence of this mutation on substrate binding and catalysis.

ACKNOWLEDGMENT

We thank Ms. Yuan Wang for excellent technical assistance in constructing the MAOA mutants.

REFERENCES

1. Brunner, H. G., Nelen, M., Breakefield, X. O., Ropers, H. H., and van Oost, B. A. (1993) *Science* 262, 578.
2. Cases, O., Seif, I., Grimsby, J., Gaspar, P., Chen, K., Pourin, S., Muller, U., Aguet, M., Babinet, C., Shih, J. C., and DeMaeyer, E. (1995) *Science* 268, 1763.
3. Weyler, W., Titlow, C. C., and Salach, J. I. (1990) *Biochem. Biophys. Res. Commun.* 173, 1205.
4. Binda, C., Coda, A., Angelini, R., Federico, R., Ascenzi, P., and Mattevi, A. (1999) *Structure* 7 (3), 265.
5. Wouters, J., and Guy, B. (1998) *Proteins: Struct. Funct. Genet.* 32 (1), 97.
6. Bach, A. W., Lan, N. C., Johnson, D. L., Abell, C. W., Bembek, M. E., Kwan, S. W., Seeburg, P. H., and Shih, J. C. (1988) *Proc. Natl. Acad. Sci. U.S.A.* 85, 4934.
7. Hsu, Y. P., Weyler, W., Chen, S., Sims, K. B., Rinehart, W. B., Utterback, M. C., Powell, J. F., and Breakefield, X. O. (1988) *J. Neurochem.* 51, 1321.
8. Hunter, C. A., and Sanders, J. K. M. (1990) *J. Am. Chem. Soc.* 112, 5525.
9. Chen, K., Wu, H. F., Grimsby, J., and Shih, J. C. (1994) *Mol. Pharmacol.* 46, 1226.
10. Bitter, G. A., and Egan, K. M. (1988) *Gene* 69, 193.
11. Nandigama, R. K., and Edmondson, D. E. (2000) *J. Biol. Chem.* 275, 20527.
12. Miller, J. R., and Edmondson, D. E. (1999) *J. Biol. Chem.* 274, 23515.
13. Miller, J. R., and Edmondson, D. E. (1999) *Biochemistry* 38, 13670.
14. Nandigama, R. K., and Edmondson, D. E. (2000) *Biochemistry* 39, 15258.
15. Walker, M. C., and Edmondson, D. E. (1994) *Biochemistry* 33, 7088.
16. Hartmann, C., and Klinman, J. P. (1991) *Biochemistry* 30, 4065.
17. Strickland, S., Palmer, G., and Massey, V. (1975) *J. Biol. Chem.* 250, 4048.
18. Hansch, C., and Leo, A. (1995) *Exploring QSAR. Fundamentals and Applications in Chemistry and Biology*, American Chemical Society, Washington, DC.
19. Bondi, A. (1964) *J. Phys. Chem.* 68, 441.
20. Barber, M. J., Eichler, D. C., Solomonson, L. P., and Ackrell, B. A. (1987) *Biochem. J.* 242, 89.
21. Klinman, J. P., and Matthews, R. G. (1985) *J. Am. Chem. Soc.* 107, 1058.
22. Fujita, T., Iwasa, J., and Hansch, C. (1964) *J. Am. Chem. Soc.* 86, 5176.
23. Hansch, C., Leo, A., and Hoekman, D. (1995) *Exploring QSAR. Hydrophobic, Electronic, and Steric Constants*, American Chemical Society, Washington, DC.
24. McEwen, C. M., Jr., Sasaki, G., and Jones, D. C. (1969) *Biochemistry* 8, 3952.